The Institution of Engineering and Technology

RPG 2022
Renewable Power Generation

22-23 September 2022

Meeting net zero carbon

Savoy Place, London

Call for papers deadline:
10 December 2021

#RPGLondon

Received: 14 July 2020 | Revised: 22 December 2020 | Accepted: 7 January 2021

IET Renewable Power Generation

DOI: 10.1049/rpg2.12110

The Institution of Engineering and Technology WILEY

ORIGINAL RESEARCH PAPER

A new method for current–voltage curve prediction in photovoltaic modules

Rafael Peña[1] | **Ana M. Diez-Pascual**[2] | **Pilar García Díaz**[1] | **Lara Velasco Davoise**[1]

[1] Department of Signal Theory and Communications, University of Alcalá, Alcalá de Henares, Spain

[2] Department of Analytical Chemistry, Physical Chemistry and Chemical Engineering, University of Alcalá, Alcalá de Henares, Spain

Correspondence
Rafael Peña, Department of Signal Theory and Communications, University of Alcalá, 28805 Alcalá de Henares, Spain.
Email: rafael.pena@uah.es

Abstract

In this work, a new method for obtaining the current–voltage curve for crystalline silicon and thin-film flat panels is presented. It is based on the single-diode model, with a variable shunt resistance and series resistance. New expressions for the shunt resistance and open circuit voltage as a function of the temperature and irradiance are deduced. Besides, a procedure to translate the series resistance to arbitrary conditions is proposed. The diode ideality factor and shunt resistance are obtained by optimization. The rest of the parameters that appear in the current–voltage curve are obtained from the module measurements by means of theoretical expressions. The procedure for obtaining the current–voltage curve under arbitrary operating conditions is also described. The results obtained with the developed model are compared with experimental measurements in cadmium telluride and amorphous silicon modules, and with results published in the literature for other technologies. The model faithfully reproduces the experimental values. For all the modules, the root mean square error for the maximum power is lower than 2% (below 1.5% in most cases). These errors are lower than those reported in the literature for other models. In particular, the results are significantly more exact in the case of thin-film modules.

1 | INTRODUCTION

In the literature, several methods to obtain the electrical parameters of commercial photovoltaic (PV) modules under arbitrary conditions of temperature and irradiance have been reported. For example, Osterwald's method (or power temperature coefficient model, PTCM) [1] is widely used due to its simplicity, since only two parameters are needed to estimate the maximum power (P_M): the temperature coefficient for power, γ, and the power of the module under reference condition, $P_{M,ref}$. Both parameters are supplied by the manufacturers in the datasheets.

PVFORM model [2, 3] enhances the results of the aforementioned method by introducing a low irradiance correction, below 125 W/m², where the PTCM overestimates the maximum power. Similarly, [3] proposes a power temperature coefficient model with correction for irradiance nonlinearity (PTCM-CIN hereinafter) that improves the ability of the former methods to represent the nonlinear behaviour at irradiances below 200 W/m².

The previous models have the advantage of requiring very few parameters for P_M estimation, but they are not very accurate, as will be shown in a following section. A more accurate method was proposed in [4]. It allows to translate the current-voltage (I–V) curve of a PV module to desired conditions of irradiance and temperature from four reference I–V curves by using bilinear interpolation (TBIM hereinafter).

The IEC 61853-3 standard [5] describes a method to calculate P_M at any irradiance and temperature by means of bilinear interpolation and extrapolation. A 23-element maximum power matrix at four different temperatures and seven different irradiances must be previously measured in order to apply the method. If the temperature or the irradiance to translate are outside the range of the measurement matrix, the IEC 61853-3 method can lead to low accuracy. This could also happen if the power matrix cannot be totally measured. Another disadvantage of the method is that it does not allow to calculate the I–V curve, so the current and voltage at maximum power point (I_M and V_M) cannot be estimated.

Other works [6–8] show algebraic models to find P_M using empirical equations that allow V_M and I_M to be approximated from open circuit voltage and short circuit current (V_{OC} and I_{SC}). In general, these equations are valid for modules of reasonable efficiency [8]. Consequently, they are more suitable for crystalline silicon (c-Si), while their use in thin-film modules can lead to significant errors.

Single-diode equivalent circuit models have been described elsewhere [9–14]. In [9], a five-parameter model is proposed, with semi-empirical equations to predict the *I–V* curve for any operating condition. It assumes a constant series resistance (R_s) and a variable shunt resistance (R_{sh}). The diode reverse saturation current, I_0, is calculated as a function of the material bandgap and cell temperature, T_C. A similar approach is described in [10], also with a constant R_s and a variable R_{sh}.

Some works have also been published about the application of the single-diode model to thin-film modules (mainly, cadmium telluride and amorphous silicon) [15–17]. For example, in [15], the single-diode model is modified by adding a dependent current source in order to take into account the higher recombination losses in these devices. Along the same lines, in [17], the model is modified with the addition of a dependent current source and considering that all the model parameters depend on the irradiance on the module.

Some authors have proposed the two-diode model to calculate the *I–V* curve of PV modules [18]. In this model, a second diode is added in parallel with the first one, which accounts for recombination losses in the junction. The ideality factor for the first diode is typically 1, while for the second one it is close to 2.

However, to obtain accurate results, it is necessary to modify, at least, the ideality factor of the second diode, making it different from 2, and dependent on the technology and material of the module.

Furthermore, it is necessary to calculate the saturation current of both diodes, adding at least one more parameter to the calculation process.

Therefore, compared to the single-diode model, the two-diode model significantly increases the complexity and the computation time. That is why most authors prefer the single-diode model. In return, the two-diode model can be more accurate, especially when calculating the *I–V* curve under low irradiance conditions.

The main objective of this work is to present a new method for obtaining the *I–V* curve for flat panels made of crystalline silicon (both monocrystalline and polycrystalline, m-Si and p-Si) and thin-films (cadmium telluride—CdTe, copper indium diselenide—CIS, and amorphous silicon—a-Si). Starting from the single-diode model, a new expression is deduced for the dependence of the shunt resistance on the irradiance. The series resistance in the developed model depends on the irradiance and temperature. The use of a variable series resistance allows to obtain higher precision compared to other single-diode models.

The procedure for obtaining the *I–V* curve under arbitrary operating conditions is also described, and a new expression is introduced to calculate V_{OC} as a function of the temperature and irradiance. Besides, a simplified procedure to transfer series resistance to arbitrary conditions is proposed.

The method proposed in this work does not require a more detailed characterization of the modules than other methods. Since series and shunt resistance are calculated from the *I–V* curves obtained under sunlight illumination, no additional measurements are required (such as dark *I–V* measurements).

2 | *I–V* CURVE IN COMMERCIAL PV MODULES

The *I–V* characteristic of a solar panel, under the single-diode model, can be expressed as:

$$I = I_L - I_0 \left[\exp\frac{V+R_s I}{N_S n k T_c/q} - 1\right] - \frac{V + IR_s}{R_{sh}} \quad (1)$$

being I_L the light-generated current, I_0 the diode saturation current, R_s the series resistance, R_{sh} the shunt resistance, n the diode ideality factor, N_S the number of cells in series in the module, k Boltzmann's constant, T_C the solar cell temperature in the module, and q the elementary charge.

In order to work with Equation (1), it is necessary to previously estimate the values of I_0, n, R_s, and R_{sh}. In addition, I_L and V_{OC} must be known, as shown in next section.

2.1 | Calculation of I_0

I_0 can be obtained by imposing open circuit conditions on the *I–V* curve:

$$0 = I_L - I_0 \exp\left[\frac{V_{OC}}{N_S n K T_c/q} - 1\right] - \frac{V_{OC}}{R_{sh}} \quad (2)$$

Then:

$$I_0 = \frac{I_L - \frac{V_{OC}}{R_{sh}}}{\exp\frac{V_{OC}}{N_s n K T_c/q} - 1} \quad (3)$$

The previous equation allows calculating I_0 if n and R_{sh} are previously estimated, assuming $I_L = I_{SC}$. Furthermore, it is necessary to know I_{SC} and V_{OC}, either experimentally or translating the values from reference condition ($T_{c,ref} = 25\ °C$, $G_{ref} = 1000\ W/m^2$), as will be shown in Section 3.1.

2.2 | R_s calculation

From Equation (1), at maximum power point:

$$I_M = I_L - I_0 \cdot \left[\exp\frac{V_M+R_s I_M}{N_S n K T_c/q} - 1\right] - \frac{V_M+I_M R_s}{R_{sh}} \quad (4)$$

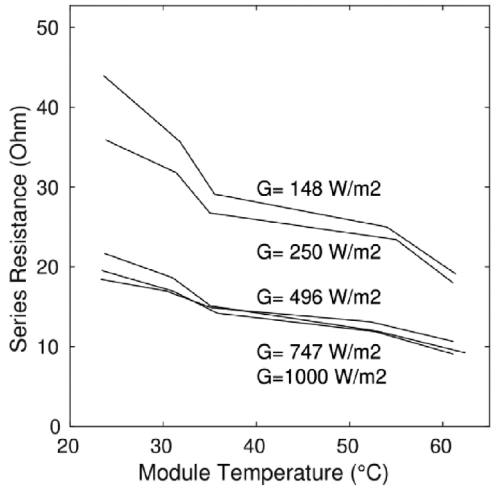

FIGURE 1 Values obtained for R_s using Equation (6) as a function of T_c for ref. [19] CdTe module

From Equation (4), the following expression can be derived:

$$R_s = \frac{N_S n K T_c/q \cdot \ln\left(\frac{I_L - I_M - \frac{V_M}{R_{sh}} - \frac{R_s I_M}{R_{sh}} + I_0}{I_0}\right) - V_M}{I_M} \quad (5)$$

R_s can be obtained from Equation (5) by iteration. Nevertheless, in practice $R_s \times I_M/R_{sh} << I_L$:

$$R_s = \frac{N_S n K T_c/q \cdot \ln\left(\frac{I_L - I_M - \frac{V_M}{R_{sh}}}{I_0} + 1\right) - V_M}{I_M} \quad (6)$$

Equation (6) can be further simplified if 1 is neglected against I_L/I_0, which is always reasonable.

R_S can be obtained from Equation (6) assuming $I_L = I_{SC}$ if n and R_{sh} are previously known.

It is important to note that R_s depends on V_M and I_M. Therefore, Equation (6) can only be used in those modules in which these parameters are known.

As can be observed, R_s depends on T_c and G. Figure 1 shows this dependency for ref. [19] CdTe module. A simplified model for R_s proposed by the authors will be shown in Section 3.2.

Equation (6) has been deduced at maximum power point. However, assuming a constant R_s in all the I–V curve leads to very accurate results. This is due to the low influence of this parameter on the performance of the module as the current decreases close to open circuit.

Good results in crystalline silicon modules (m-Si or p-Si) are obtained by assuming a constant R_s, as most authors do. However, this approach does not lead to accurate results in thin-film modules.

2.3 | Estimation of n and R_{sh}

The estimation of n and R_{sh} departs from the realization of a set of measurements for each module at different temperatures and irradiances. The experimental values for I_M, V_M, I_{SC}, V_{OC}, and P_M under different operating conditions are required. From these data, it is possible to obtain the I–V curve for different values of n and R_{sh} using Equation (1), and using Equation (6) to calculate R_s. Subsequently, P_M can be estimated from the I–V curve, upon finding the maximum value for the product $I \times V$.

The values chosen for n and R_{sh} are those for which the root mean square error (RMSE) for the calculated P_M is minimum compared to the experimental measurements. Therefore, with this method, no additional measurements are required to obtain n and R_{sh}.

As will be shown below, assuming a constant n provides good results. Conversely, assuming a constant R_{sh} leads to significant error, since R_{sh} increases with decreasing irradiance [9–11].

In this regard, very good results are obtained with the following empirical expression, developed by the authors:

$$R_{sh} = R_{sh,ref}\left[1 + k_{Rsh}\left(G_{Rsh} - G\right)\right] \quad \text{for} \quad G < G_{Rsh} \quad (7a)$$

$$R_{sh} = R_{sh,ref} \quad \text{for other } G \quad (7b)$$

being $R_{sh,ref}$ the shunt resistance at reference condition and G_{Rsh} and k_{Rsh} the two dependency parameters in the model, measured in W/m² and in m²/W, respectively.

G is the effective irradiance, that is, the one which would be measured with a reference cell with the same spectral and angular response. Once the short-circuit current is known under the reference condition, the effective irradiance is obtained from the module I_{SC} and the temperature coefficient α, assuming that I_{SC} varies linearly with the irradiance:

$$G = I_{SC}\frac{G_{ref}}{I_{SC,ref}\left[1 + \text{ff}\left(T_c - T_{c,ref}\right)\right]} \quad (8)$$

It is important to use the effective irradiance in the characterization of the modules in order to avoid the effects of variations in solar spectrum and reflectance losses [9, 20]. In particular, in a-Si modules these effects could be significant.

As shown above, the parameters $R_{sh,ref}$, k_{Rsh}, and G_{Rsh}, in addition to n, are obtained by optimization. i.e. their value corresponds to the minimum RMSE for the calculated P_M.

Equation (7a) can be simplified by assuming a constant G_{Rsh}, regardless of the module technology. In this regard, it has been found that $G_{Rsh} = 550$ W/m² leads to very good results in all the measured modules. Hereinafter, this value will be taken for all the calculations. With this assumption, R_{sh} just depends on two parameters.

Assuming a constant k_{Rsh} value of 0.0064 m²/W also provides very good results for all technologies. Therefore, Equation (7a) can be written as:

$$R_{sh} = R_{sh,ref}\left[1 + 0.0064\left(550 - G\right)\right] \quad \text{for } G < G_{Rsh} \quad (9)$$

The k_{Rsh} value of 0.0064 m²/W used in Equation (9) is an average of the optimum values for the different technologies shown in Section 4.3.

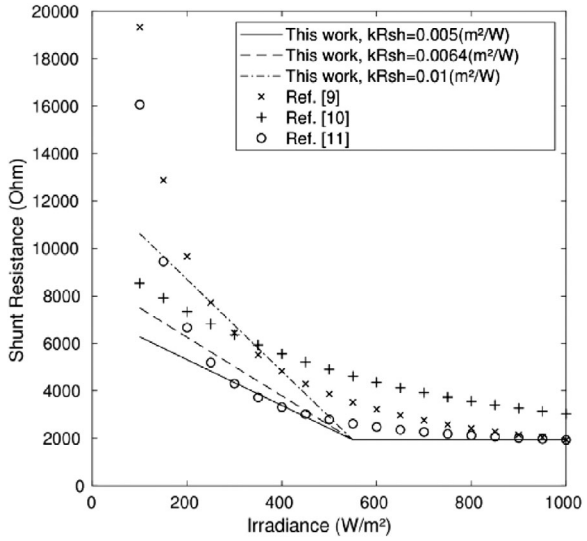

FIGURE 2 R_{sh} values obtained with Equation (9) and those obtained with the expressions in [9–11] as a function of irradiance. For Equation (9), k_{Rsh} has been fixed to 0.005, 0.0064 m²/W and to 0.01 m²/W. $R_{sh,ref}$ has been fixed to 1932 Ω, as in [11]

Equation (9) will not be used hereinafter, though it could be used if a very simple expression for R_{sh} is searched. It is only included for the sake of completeness.

The proposed equations for R_{sh} as a function of G have been compared to the expressions proposed in other works. In this sense, it has been proven that better results are obtained with Equations (7a) and (7b) than with the expressions described in [9–11]. Therefore, in the results section, Equations (7a) and (7b) have been used, with very accurate results (see Section 4.4).

Figure 2 shows the R_{sh} values obtained with Equations (7a) and (7b) and those obtained with the expressions in [9–[11] as a function of irradiance. In the figure, the values obtained for k_{Rsh} = 0.005 m²/W, k_{Rsh} = 0.0064 m²/W, and k_{Rsh} = 0.01 m²/W are presented, in order to show the influence of this parameter. $R_{sh,ref}$ has been fixed to 1932 W, as in [11]. It can be seen that [9–11] expressions lead to higher R_{sh} values at middle and high irradiance. And that [10] and [11] expressions lead to very high R_{sh} values at low irradiance.

3 | TRANSLATION TO ARBITRARY IRRADIANCE AND TEMPERATURE CONDITIONS

To obtain the module I–V curve under arbitrary temperature and irradiance conditions, the formerly calculated values for n, $R_{sh,ref}$, and k_{Rsh} are used. I_0 can be estimated using Equation (3) if V_{OC} and I_{SC} under the conditions to be translated (T_c and G) are previously known. The details of the calculations are shown below.

3.1 | V_{OC} and I_{SC} translation: Calculation of the temperature coefficients

In order to calculate V_{OC} from the value under the reference condition, $V_{OC,ref}$, the following empirical expression is proposed herein:

$$V_{OC} = V_{OC,ref}\left[1+\beta\left(T_c - T_{c,ref}\right)\right]\left[1+k_G N_S \frac{kT_c}{q}\ln\left(G/G_{ref}\right)\right] \tag{10}$$

where β and k_G are the temperature coefficient and the irradiance correction coefficient for V_{OC}, respectively. These parameters are calculated as those values for which the RMSE for the estimated V_{OC} is minimum with regard to the experimental values.

Equation (10) complies a trade-off between simplicity and accuracy. As will be shown later, very low RMSEs are obtained, and only two fitting parameters are required.

Regarding I_{SC}, very good results are achieved by using the well-known expression:

$$I_{SC} = I_{SC,ref}\frac{G}{G_{ref}}\left[1+\alpha\left(T_c - T_{c,ref}\right)\right] \tag{11}$$

being α the temperature coefficient for I_{sc} and $I_{SC,ref}$ the short circuit current at reference condition.

It is important to use experimental temperature coefficients, instead of those found in the manufacturer's datasheet [21]. Due to the tolerance in the manufacturing processes, very important deviations in the actual value of the coefficients are found for different modules of the same technology.

3.2 | R_s translation to arbitrary temperature and irradiance conditions

It is not possible to calculate R_s as a function of T_c and G from Equation (6), since it depends on V_M and I_M. These last two parameters are not known a priori under the desired conditions of irradiance and temperature.

This problem can be solved by having a broad set of experimental values for the electrical parameters of the modules. R_s can be obtained as a function of irradiance and temperature from these data. To translate R_s, the closest available values can be selected and a bilinear interpolation can be performed. However, it is not necessary to do so if the following procedure proposed by the authors is applied.

Firstly, three values for R_s are calculated, under reference condition, at G = 800 W/m² and T_c = NOCT and at low irradiance:

$$R_{s,ref} = R_s(G = 1000\ \text{W/m}^2, \quad T_c = 25\ °\text{C}) \tag{12a}$$

$$R_{s,NOCT} = R_s\left(G = 800\ \text{W/m}^2, \quad T_c = \text{NOCT}\right) \tag{12b}$$

$$R_{s,low} = R_s(G = 200\ W/m^2, \quad T_c = 25\ °C) \tag{12c}$$

being NOCT the nominal operating cell temperature in the module.

In Equations (12a), (12b), and (12c), $R_{s,ref}$, $R_{s,NOCT}$, and $R_{s,low}$ are calculated from Equation (6), using the experimental values of V_M and I_M previously measured.

Then, R_s can be estimated using the following empirical expressions:

$$R_s = R_{s,ref} + 0.92\frac{R_{s,NOTC} - R_{s,ref}}{NOCT - T_{c,ref}}\left(T_c - T_{c,ref}\right) \quad \text{for} \quad G \geq 300\ W/m^2 \tag{13a}$$

$$R_s = R_{s,low} + \frac{1.48R_{s,ref} - R_{s,low}}{57 - T_{c,low}} \cdot \left(T_c - T_{c,low}\right) \quad \text{for} \quad G < 300\ W/m^2 \tag{13b}$$

being $T_{c,low} = 25\ °C$ and using the NOCT provided by the manufacturer in the datasheet.

The expressions for R_s in Equations (13a) and (13b) have been deduced by the authors by means of an exhaustive analyses of the experimental measurements. The starting point for obtaining the equations has been a linear regression between the three conditions that appear in Equations (12a), (12b), and (12c). The expressions obtained with this linear regression have been modified in order to minimize the error for the modules of all the considered technologies under the different conditions of irradiance and temperature.

They are applicable, at least, to all the technologies studied in this work: m-Si and p-Si and CdTe, CIS, and a-Si PV modules.

Equations (13a) and (13b) show that the variation of R_s with T_c is different for low G than for medium and high G. This can be seen in Figure 3, which shows the R_s values calculated as a function of T_c. $R_{s,ref}$ has been fixed to 18 Ω.

Equations (13a) and (13b) have been compared to the expression proposed in [12], in which R_s depends exponentially on T_c through a temperature coefficient. The values for R_s obtained with that expression have been depicted in Figure 3, in which the temperature coefficient for R_s has been fitted in order to minimize the error in R_s at high irradiance. It can be seen that the exponential expression in [12] provides very similar results to Equation (13a). Nevertheless, no variation with G is considered in [12] for R_s. Therefore, the exponential variation cannot reproduce the R_s values at low irradiance.

As will be shown later, Equations (13a) and (13b) lead to very accurate results for the calculation of the I–V curve for the wide range of irradiances and temperatures considered in this work. In this sense, the validity of the equations has been tested for T_c between 25 and 63 °C and for G between 130 and 1080 W/m^2.

It is worth commenting that the conditions chosen to calculate R_s in Equations (13a) and (13b) are those for which most manufacturers supply the electrical parameters of the modules in the datasheets. Although not every manufacturer provides the values at 25 °C and 200 W/m², there is a tendency to include them lately.

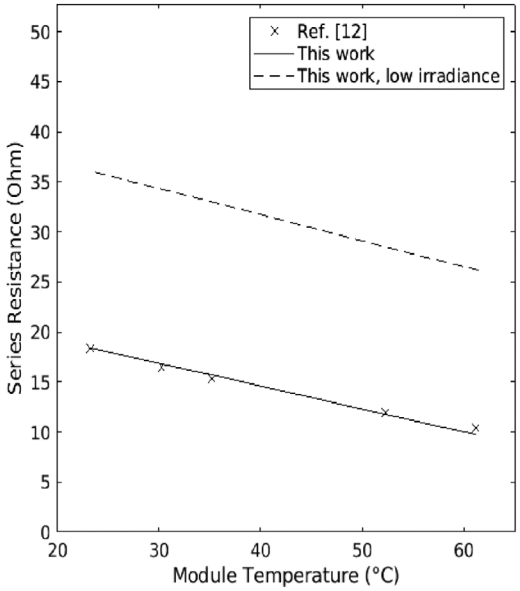

FIGURE 3 R_s values obtained with Equation (13a) and (13b) and those obtained with the expression in [12] as a function of temperature. The solid line corresponds to R_s values for G higher than 300 W/m², while the dashed line corresponds to G lower than 300 W/m². $R_{s,ref}$ has been fixed to 18 Ω

If the experimental values for the electrical parameters of the module are only available under reference condition and for $G = 800$ W/m², the following expressions also provide very good results:

$$R_s = R_{s,ref} + 0.92\frac{R_{s,NOTC} - R_{s,ref}}{NOCT - T_{c,ref}} \cdot \left(T_c - T_{c,ref}\right) \quad \text{for} \quad G \geq 300\ W/m^2 \tag{14a}$$

$$R_s = 2R_{s,ref} \quad \text{for} \quad G < 300\ W/m^2 \tag{14b}$$

3.3 | Application of the method with a limited set of data

The proposed method can also be applied in case only a limited set of experimental measurements are available. The way to obtain the parameters through optimization allows to do it. For instance, the method can be applied measuring the electrical parameters under reference condition, at $G = 800$ W/m² and $T_c =$ NOCT and at low irradiance and using Equations (13a) and (13b).

Even without the electrical parameters at low irradiance, it can be applied using Equations (14a) and (14b). The values of n and $R_{sh,ref}$ can be obtained as shown in Section 2.3, calculating the values that minimizes the RMSE in P_M for all the measured values. In this way, it is not necessary to make detailed measurements under specific conditions, obtaining a certain maximum power matrix.

The method can also be applied with the datasheet parameters at reference condition, at 800 W/m^2 and at low irradiance, at the expense of a lower accuracy. In this case, Equation (9) provides accurate results for R_{sh} calculation, leading to a very simple model. This approach can be useful for engineering purposes, in the design phase of PV plants.

4 | RESULTS

A measurement campaign has been carried out for two commercial a-Si and CdTe modules, throughout the year 2019, on the campus of the University of Alcalá (UAH), in Madrid. During this period, module in-plane irradiance values from slightly above 100 W/m² to over 1100 W/m² have been recorded. Only the measurements obtained on clear days have been processed, in which the stability in the irradiance and temperature values during the measurements is guaranteed. Regarding the ambient temperature, values from −3 °C to about 40 °C have been registered.

This wide range of environmental conditions is more than enough to carry out an exhaustive characterization of the presented model in the two measured modules. In this sense, the electrical parameters of the modules (including I_{SC}, V_{OC}, P_M, I_M, and V_M) have been measured for T_c between 25 and 60 °C and for G between 100 and 1000 W/m^2. The results are shown in Tables A1 and A 2 (Appendix 1).

4.1 | Calculation of $I_{SC,ref}$ and α

In order to calculate α and $I_{SC,ref}$, a high precision pyranometer (secondary standard) has been used. The measurements have been made with natural light (outdoors), placing the pyranometer in the same plane as the module. The temperature has been measured by placing two type k-thermocouples on the back of the panel, perfectly joined to it by thermal insulating putty. In addition, the ambient temperature has been measured in the plane of the panels.

The procedure used is as follows. Firstly, I_{SC} is measured at 1000 W/m² and T_c close to 25 °C. The measurement is made by placing the panel perpendicular to the sun with the pyranometer in the same plane. It is always essential to check the irradiance stability.

To carry out this measurement, a cold and clear day was chosen at the end of February, with an ambient temperature between −2 and 5 °C throughout the morning. After reaching the irradiance level of 1000 W/m² in the plane of the panel, I_{SC} was measured at a temperature close to 25 °C for the a-Si module and the CdTe module. It is not necessary to measure exactly at the reference condition, since $I_{SC,ref}$ can be obtained by regression from the coefficient α, as shown below.

Furthermore, it is necessary to measure I_{SC} for T_c between 30 and 60 °C in order to calculate α. To set these temperatures, a 9 kW industrial heater was used. The heater fan was kept away from the plane of the panels, allowing the heating area to be much larger than the panel surface, ensuring temperature uniformity. This uniformity has been verified experimentally, by means of four thermometers located around the measurement plane (Figure 4).

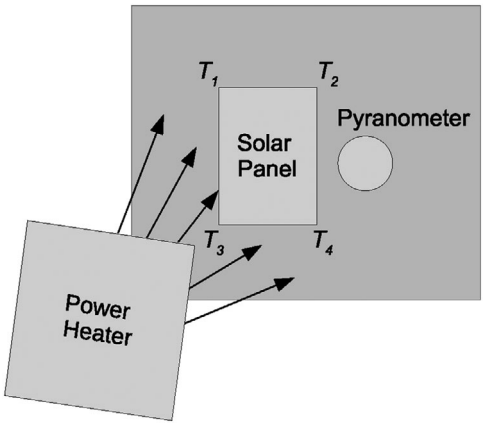

FIGURE 4 Experimental setup used to measure the short-circuit current and the temperature coefficient for I_{SC}. Irradiance is measured with a pyranometer in the plane of the panels. Temperature can be increased by means of an industrial power heater. Temperature uniformity is checked by means of 4 thermometers around the module. The figure does not show two thermocouples attached to the rear face of the module

To increase the temperature in the panel, it is possible to regulate the power and air flow of the heater. It is important to preheat the area where the module is located to ensure thermal uniformity.

$I_{SC,ref}$ and α are obtained by finding those values that minimize the RMSE for the I_{SC} measurements against T_c at 1000 W/m² with respect to the estimation with Equation (11). Table A3 (Appendix 1) shows the parameters obtained for the two modules characterised together with the RMSE, expressed as a percentage of the average I_{SC}. As it can be observed, the error is very low in both cases, with values of 0.88% and 0.56%, respectively.

Likewise, the theoretical and experimental values are shown in Figures 5 and 6. The figures include a diagonal line with slope one. Data above this line correspond to values overestimated by the model, while those below correspond to data for which the model predicts an I_{SC} lower than the measured value.

4.2 | Calculation of $V_{OC,ref}$, β, and k_G

According to Equation (10), V_{OC} depends on three parameters, $V_{OC,ref}$, β, and k_G. These parameters are obtained by optimisation: those values that minimise the RMSE for the estimated V_{OC} compared to the experimental measurements are chosen. It is important to notice that the temperature of the rear face of the module is considered here. And the effective irradiance on the panel is calculated according to Equation (8).

Figures 7 and 8 show the measurements made for V_{OC} and the value estimated using Equation (10) for the two modules characterised in our laboratory. The values for the three

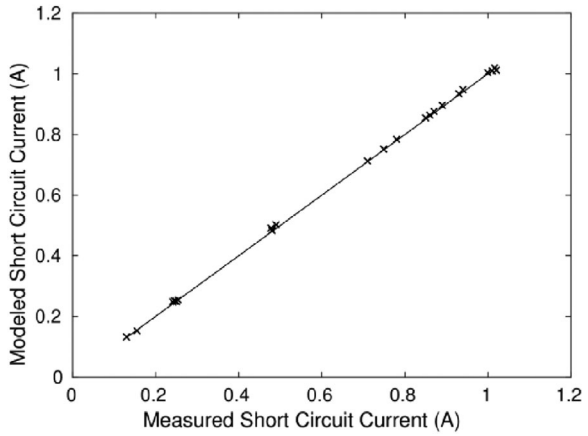

FIGURE 5 Values obtained for I_{SC} as a function of the experimental values for the a-Si module. The figure includes a diagonal line with slope one. Values above this line are overestimated by the model, while those below correspond to data for which the model predicts an I_{SC} lower than measured

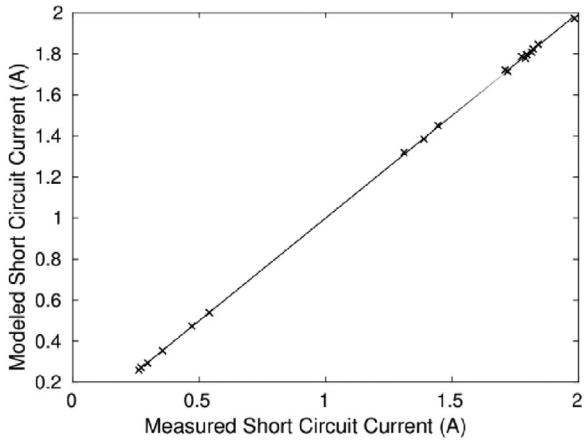

FIGURE 6 Values obtained for I_{SC} as a function of the experimental values for the CdTe module

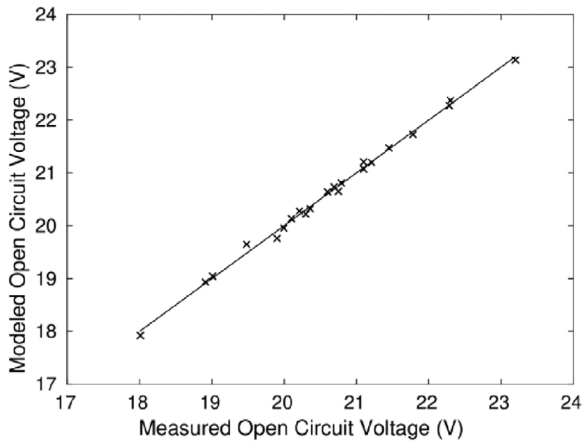

FIGURE 7 Values obtained for V_{OC} as a function of the experimental values for the a-Si module

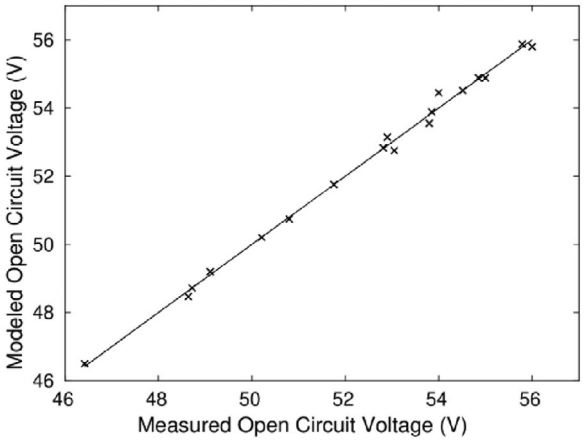

FIGURE 8 Values obtained for V_{OC} as a function of the experimental values for the CdTe module

parameters and the RMSEs expressed as a percentage of the average V_{OC} are shown in Table A3. It can be observed that the results are very satisfactory, the RMSE is lower than 0.5% in the two modules.

4.3 | Calculation of n, $R_{sh,ref}$, and k_{Rsh}

As previously mentioned, these three parameters are obtained by optimisation. The values for which the RMSE for the calculated P_M is minimum with respect to the experimental measurements are taken. I_0 and R_s must be previously calculated in order to obtain P_M. It is important to note that the R_s used herein is that obtained with Equation (6), from the experimental values of I_{SC}, V_{OC}, I_M, and V_M (although R_s does not explicitly depend on V_{OC}, it does depend on I_0, for which V_{OC} is required).

In order to obtain the values of the current for each voltage in the I–V curve, three different numerical methods have been tested: fixed point iteration, Newton–Raphson, and bisection methods. The last two procedures give fewer convergence problems than the first one. The latter has been finally chosen, as it is the most robust in ensuring convergence.

Table A4 (Appendix 1) shows the optimum values for the three model parameters for the two modules characterized by the authors and for six modules of the reference [19]. The RMSEs for P_M with respect to the experimental values are also included. They are expressed as a percentage of the average P_M.

It can be observed that the values for n are consistent with those expected for each technology [22–24]. In the case of the CdTe modules, that of UAH has $n = 1.5$, compared to 1.8 for that of [19]. However, for n between 1.5 and 1.8, the error in these modules is very low. Therefore, either of the two values leads to very similar results.

Regarding the a-Si modules, n depends on the number of junctions. The calculated values are in the range 1.6–1.8 per junction, as expected according to the literature.

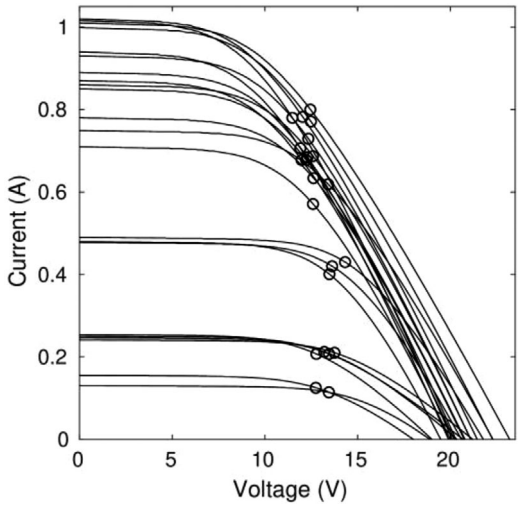

FIGURE 9 Modelled *I–V* curves for the a-Si module. The experimental maximum power point is also displayed on each curve by means of a circle

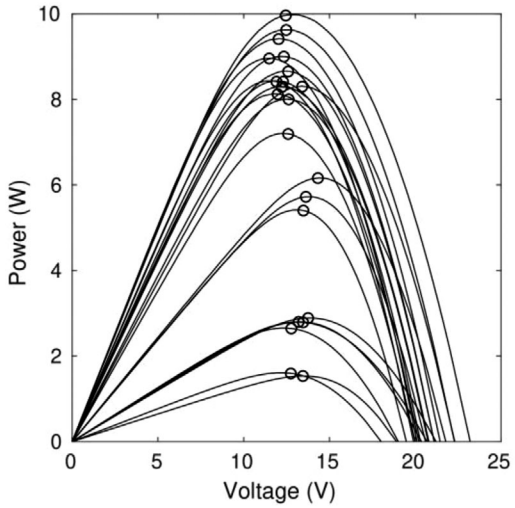

FIGURE 11 Modelled *P–V* curves for the a-Si module. The experimental maximum power point is also displayed on each curve by means of a circle

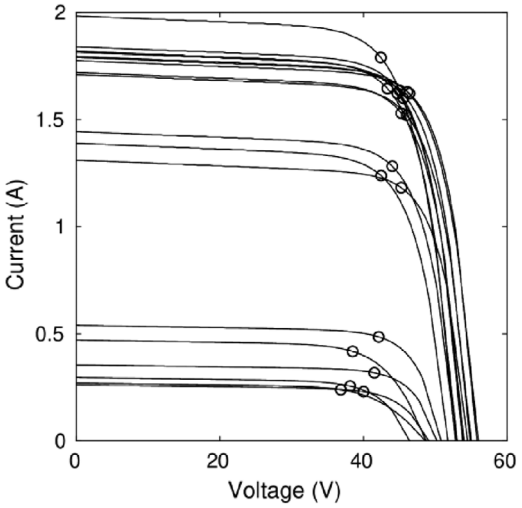

FIGURE 10 Modelled *I–V* curves for the CdTe module. The experimental maximum power point is also displayed on each curve by means of a circle

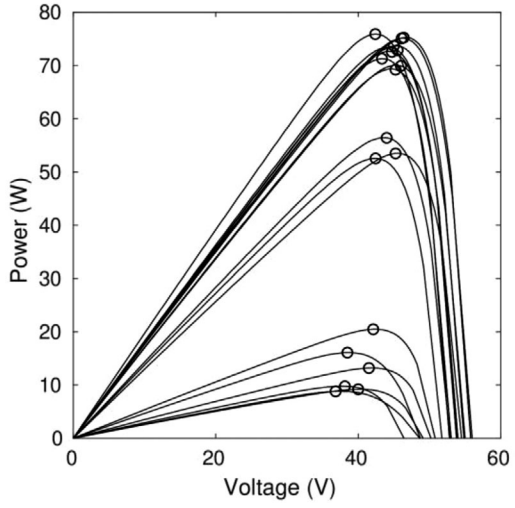

FIGURE 12 Modelled *P–V* curves for the CdTe module. The experimental maximum power point is also displayed on each curve by means of a circle

It is found that the results are very satisfactory. RMSE is below 0.3% for the two modules measured. With regard to the modules characterised by other authors [19], RMSE is systematically lower than 0.7%, being in most cases below 0.5%.

These results could be improved by taking the optimum value for each module for G_{Rsh} (fixed at 550 W/m² in Table A4). However, this is not necessary given the low errors obtained.

Figures 9–12 show the modelled *I–V* and *P–V* curves for the two modules characterised in the UAH. In order to compare with the experimental results, the figures include the measured values for the maximum power point of the modules at every irradiance and temperature.

It can be seen that, as expected according to the low RMSEs obtained (Table A4), the measured values are very close to those provided by the model.

4.4 | Calculation of the *I–V* curve under arbitrary irradiance and temperature conditions

Once the model parameters have been obtained, it is possible to calculate the *I–V* curve of the modules under arbitrary irradiance and temperature conditions.

For this purpose, I_{SC} and V_{OC} are firstly calculated with the coefficients obtained in 4.1 and 4.2. Then, I_0 is calculated using Equation (3) and R_s using Equations (13a) and (13b), for each value of T_c and G.

The results obtained with the model have been compared with the experimental measurements carried out and with those provided in [19]. Figures 13 and 14 show the measurements made for P_M and the estimated values for the two modules characterized in our laboratory. Table A5 shows the RMSE obtained for P_M for the eight modules considered. Both the errors using

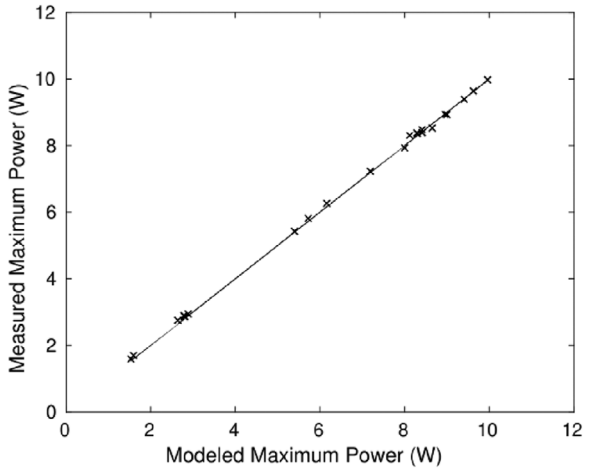

FIGURE 13 Values obtained for P_M as a function of the experimental values for the a-Si module

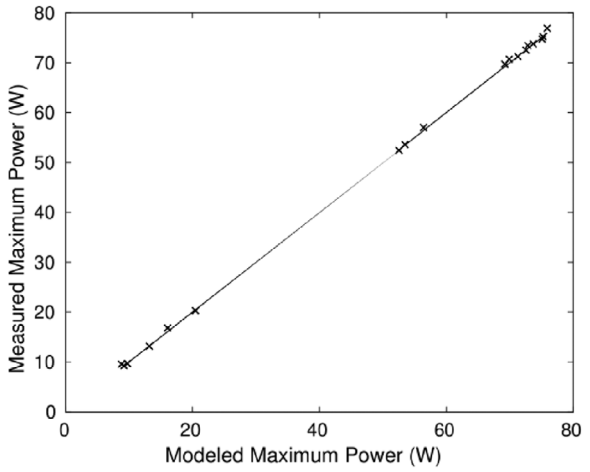

FIGURE 14 Values obtained for P_M as a function of the experimental values for the CdTe module

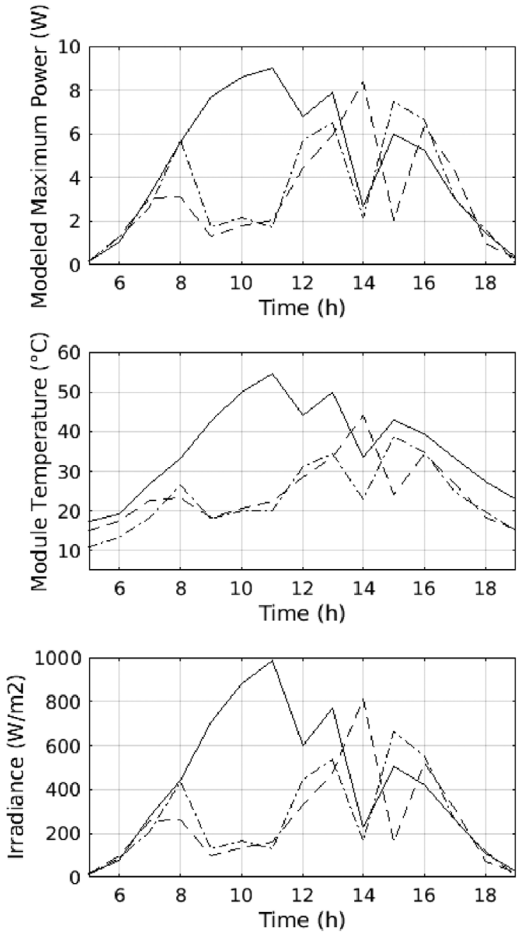

FIGURE 15 Irradiance, module temperature and modelled maximum power for the a-Si module as a function of time. The displayed values correspond to three different days in the middle of June

Equations (13a) and (13b) for R_s and those obtained with Equations (14a) and (14b) are shown. The RMSE obtained calculating P_M with the Osterwald method (PTCM) is also included.

It can be observed that the model faithfully reproduces the experimental values of P_M for the considered irradiance and temperature range. For all the modules, the RMSE is lower than 2%, being below 1.5% in most cases. Both the full expression and the two-parameter expression for R_s gives errors in this range. The improvement by using Equations (13a) and (13b) is small, hence both expressions can be used in practice.

Table A6 shows the optimum values for the three model parameters obtained applying the method as described in Section 3.3 for the two modules characterized in the UAH. The RMSEs for the estimated P_M are also included.

In the table, n, $R_{sh,ref}$ and k_{Rsh} have been obtained calculating the values that minimizes the RMSE in P_M for the measured values under reference condition, at $G = 800$ W/m² and T_c = NOCT and at low irradiance; and using Equations (13a) and (13b). G_{Rsh} has been set at 550 W/m². Then, P_M has been calculated for all the irradiance and temperature conditions shown in Tables 1 and 2.

It can be seen that the values obtained for the model parameters and for the RMSEs (lower than 1.3% in both modules) are very similar to those calculated using the model parameters estimated from all the experimental measurements.

Figures 15 and 16 show the evolution with time of the irradiance, module temperature, modelled maximum power, and modelled voltage at maximum power point for the a-Si module. The displayed values correspond to three different days in the middle of June. The values for ambient temperature and irradiance have been obtained from PVGIS database. The module temperature has been calculated from the module NOCT.

It can be seen that the presented model allows calculating the electrical parameters of the modules for a certain time interval, including the values for V_M and I_M. This is an important advantage compared to other models, such as the PCTM, which cannot provide the values for the currents and voltages in the I–V curve. In order to size the inverter in a PV plant, it is essential to know the PV generator output voltage, which must be within the range of maximum power point tracking of the inverter.

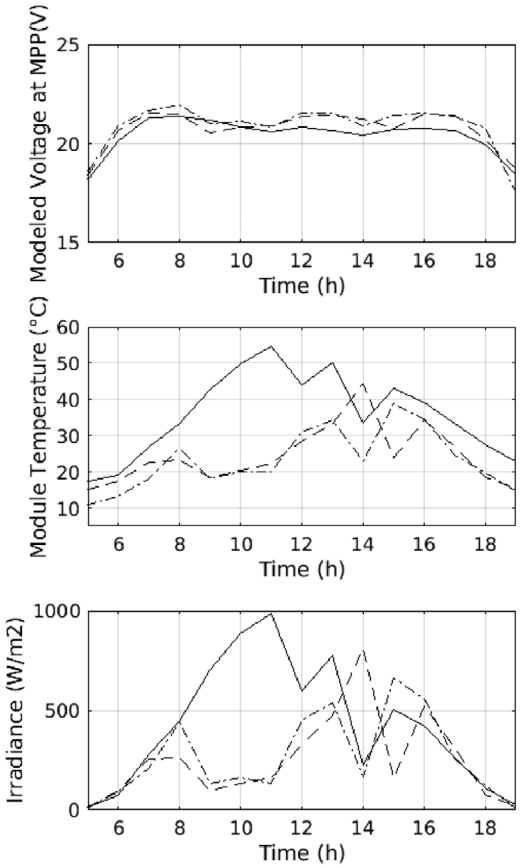

FIGURE 16 Irradiance, module temperature and modelled voltage at maximum power point for the a-Si module as a function of time. The displayed values correspond to three different days in the middle of June

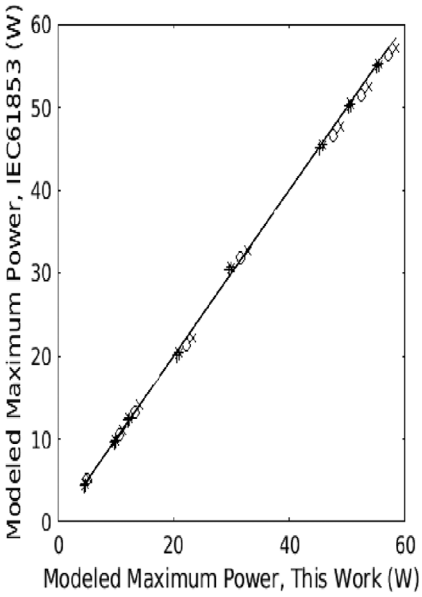

FIGURE 17 Values obtained for P_M with the IEC61853 procedure as a function of those obtained in this work for [19] CdTe module. The figure includes a diagonal line with slope one. Values above this line are overestimated by the IEC61853 procedure while those below the line are underestimated

And, in off-grid systems, in which a bank of batteries must be charged by means of the PV generator, the output voltage of the modules must be known, since it must be over the system voltage.

In order to compare the proposed method with the values provided by the one described in the IEC61853 standard, P_M has been calculated with both procedures at $G = 100$, 200, 250, 400, 600, 900, 1000, and 1100 W/m^2 and $T_c = 20$, 35, 55, and 60 °C. These irradiance and temperature conditions include values within the range of those experimentally measured and also outside that range.

The results are shown in Figure 17. It can be seen how both methods provide very similar results, except when T_c and G are outside the range of the measurement matrix. This happens for $G = 1100$ W/m^2 and for $T_c = 20$ °C. In Figure 17, this is the reason for the higher discrepancy at high P_M. In this range, errors up to 3% are observed for IEC61853 values, while values below 1% are obtained in the rest of the cases.

The RMSEs obtained when calculating P_M with the developed model are lower than those obtained with other methods. With regard to the PTCM, the average for the RMSE of all the modules is 3.15%, compared to 1.24% for the method proposed here. It is worth noting that the PCTM gives large errors in thin-film modules, above 3% for a-Si and CIS.

With regard to former published works, in [4], an average RMSE for seven modules of different technologies of 1.4% was obtained for TBIM. Or in [3], RMSEs for the PVFORM model in the range between 1.9% and 4.9% are calculated, depending on the technology of the module. In the same reference, RMSEs for the PTCMCIN are between 1.1% and 4.4%.

With regard to other methods based on the single-diode model, the results obtained herein clearly improve those of [9], where RMSEs over 5% are reported even for single P_M measurements (at a specific irradiance and temperature) for the two characterised thin-film modules. With respect to those published in [10], the RMSEs for crystalline silicon modules are similar, while those for CIS modules are higher than in this work. Nonetheless, the number of measurements in the aforementioned work is much higher, making the comparison difficult.

The model presented herein also provides very good results at low irradiance. This, together with the lower number of parameters required, makes it preferable compared to those models based on two diodes, in the authors' opinion.

5 | SUMMARY AND CONCLUSIONS

A method to obtain the I–V curve for c-Si and thin-film PV modules has been developed in this work. It is based on the single-diode model, with a variable shunt resistance and series resistance. A new expression for the shunt resistance, which depends on the irradiance, has been deduced.

The diode ideality factor and shunt resistance are obtained by optimization. The rest of the parameters that appear in the I–V curve equation (I_0 and R_s) are obtained from the PV module measurements by means of theoretical expressions.

Measurements are also required to calculate the temperature coefficients for I_{SC} and for V_{OC}, as well as $I_{SC,ref}$ and $V_{OC,ref}$.

The procedure for obtaining the I–V curve under arbitrary operating conditions has also been described. A new expression has been introduced to calculate V_{OC} from temperature and irradiance. Besides, a simplified procedure to transfer the series resistance to arbitrary conditions is proposed.

The results obtained with the developed model have been compared with experimental values for CdTe and a-Si modules, and with experimental results published in the literature for other technologies.

The model faithfully reproduces the experimental values. For all the modules, the RMSE for P_M under different operating conditions is lower than 2%, being below 1.5% in most cases. These values are lower than those reported in the literature for other models. In particular, the model clearly improves the results for thin-film modules.

Compared to other procedures for calculating the electrical parameters of PV modules under arbitrary operating conditions, working with the I–V curve allows obtaining V_M and I_M. Furthermore, the developed model does not require to carry out specific measurements to obtain n and R_{sh}, apart from the electrical characterisation of the modules at different temperatures and irradiances. Finally, the proposed method is valid for all flat panel technologies that have been tested.

ACKNOWLEDGMENTS

Action financed by the Community of Madrid within the framework of the multi-year agreement with the University of Alcalá in the line of action "Stimulus to Excellence for University Permanent Professors", ref. EPU-INV/2020/012.

REFERENCES

1. Osterwald, C.R.: Translation of device performance measurements to reference conditions. Sol. Cells 18(3), 269–279 (1986)
2. Menicucci, D.F.: Photovoltaic array performance simulation models. Sol. Cells 18(3), 383–392 (1986)
3. Marion, B.: Comparison of predictive models for photovoltaic module performance. In: 33rd IEEE Photovoltaic Specialists Conference. San Diego, CA pp. 1–6 (2008)
4. Marion, B., Rummel, S., Anderberg, A.: Current–voltage curve translation by bilinear interpolation. Prog. Photovoltaics Res. Appl. 12(8), 593–607 (2004)
5. IEC61853-3: PV module performance testing and energy rating - Part 3: Energy rating of PV modules. International Electrotechnical Commission (IEC), Geneva (2018)
6. Fuentes, M., et al.: Application and validation of algebraic methods to predict the behaviour of crystalline silicon PV modules in Mediterranean climates. Sol. Energy 81(11), 1396–1408 (2007)
7. Green, M.A.: Solar Cells: Operating Principles, Technology, and System Applications. Prentice-Hall, Inc., Englewood Cliffs, NJ, p. 288 (1982)
8. la Parra, I., et al.: PV performance modelling: A review in the light of quality assurance for large PV plants. Renewable Sustainable Energy Rev. 78, 780–797 (2017)
9. De Soto, W., Klein, S.A., Beckman, W.A.: Improvement and validation of a model for photovoltaic array performance. Sol. energy 80(1), 78–88 (2006)
10. Mermoud, A., Lejeune, T.: Performance assessment of a simulation model for PV modules of any available technology. In: Proceedings of the 25th European Photovoltaic Solar Energy Conference. Valencia, Spain (2010)
11. Dobos, A.P., MacAlpine, S.M.: Procedure for applying IEC-61853 test data to a single diode model. In: IEEE 40th Photovoltaic Specialist Conference (PVSC). Denver, CO, pp. 2846–2849 (2014)
12. Boyd, M.T., et al.: Evaluation and validation of equivalent circuit photovoltaic solar cell performance models. J. Sol. Energy Eng. 133(2), 021005 (2011)
13. Elazab, O.S., et al.: Parameters estimation of single- and multiple-diode photovoltaic model using whale optimisation algorithm. IET Renewable Power Gener. 12(15), 1755–1761 (2018)
14. Wang, Y., Hsu, P.: Analytical modelling of partial shading and different orientation of photovoltaic modules. IET Renewable Power Gener. 4(3), 272–282 (2010)
15. Merten, J., et al.: Improved equivalent circuit and analytical model for amorphous silicon solar cells and modules. IEEE Trans. Electron Devices 45(2), 423–429 (1998)
16. Merten, J., et al.: The role of the buffer layer in the light of a new equivalent circuit for amorphous silicon solar cells. Sol. Energy Mater. Sol. Cells 57(2), 153–165 (1999)
17. Lineykin, S., Averbukh, M., Kuperman, A.: Issues in modeling amorphous silicon photovoltaic modules by single-diode equivalent circuit. IEEE Trans. Ind. Electron. 61, 6785–6793 (2014)
18. Humada, A.M., et al.: Solar cell parameters extraction based on single and double-diode models: A review. Renewable Sustainable Energy Rev. 56, 494–509 (2016)
19. Marion, B., et al.: Validation of a photovoltaic module energy ratings procedure at NREL. National Renewable Energy Laboratory, Golden, CO (1999)
20. Klise, K.A., Hansen, C.W., Stein, J.S.: Dependence on geographic location of air mass modifiers for photovoltaic module performance models. In: IEEE 42nd Photovoltaic Specialist Conference (PVSC). New Orleans, pp. 1–5 (2015)
21. Ponce-Alcántara, S., et al.: A statistical analysis of the temperature coefficients of industrial silicon solar cells. Energy Procedia 55, 578–588 (2014)
22. Meyer, E.L.: Extraction of saturation current and ideality factor from measuring *VOC* and *ISC* of photovoltaic modules. Int. J. Photoenergy 2017, 1 (2017)
23. Cuce, P.M., Cuce, E.: A novel model of photovoltaic modules for parameter estimation and thermodynamic assessment. Int. J. Low-Carbon Technol. 7(2), 159–165 (2012)
24. Bashahu, M., Nkundabakura, P.: Review and tests of methods for the determination of the solar cell junction ideality factors. Sol. Energy 81(7), 856–863 (2007)

How to cite this article: Peña R, Diez-Pascual AM, Díaz PG, Davoise LV. A new method for current–voltage curve prediction in photovoltaic modules. *IET Renew Power Gener.* 2021;15:1331–1343. https://doi.org/10.1049/rpg2.12110

APPENDIX 1

TABLE A1 Experimental values obtained for I_{SC}, V_{OC}, P_M, I_M, and V_M as a function of G and T_c for the a-Si module

G [W/m²]	T_c [°C]	I_{SC} [A]	V_{OC} [V]	P_M [W]	I_M [A]	V_M [V]
1001	59.9	1.02	20.1	8.96	0.78	11.5
1002	44.7	1.02	21.5	9.40	0.78	12.0
999	35.6	1.00	22.3	9.62	0.77	12.5
1010	26.0	1.01	23.2	9.96	0.80	12.5
929	63.0	0.94	19.9	8.41	0.71	11.9
882	57.0	0.89	20.3	8.41	0.68	12.3
862	56.0	0.87	20.2	8.12	0.68	12.0
844	49.6	0.85	20.8	8.29	0.68	12.2
854	46.8	0.86	21.1	8.65	0.69	12.6
924	46.5	0.93	21.1	9.00	0.73	12.3
701	56.5	0.71	20.0	7.19	0.57	12.6
774	50.1	0.78	20.8	8.00	0.63	12.6
750	30.0	0.75	22.3	8.30	0.62	13.4
476	54.0	0.48	19.5	5.40	0.40	13.5
487	43.0	0.48	20.6	5.72	0.42	13.6
501	31.0	0.49	21.8	6.15	0.43	14.3
251	51.0	0.25	19.0	2.65	0.21	12.8
249	36.1	0.25	20.4	2.79	0.21	13.2
248	31.3	0.25	20.7	2.79	0.21	13.5
248	26.0	0.24	21.2	2.88	0.21	13.8
150	56.0	0.15	18.0	1.59	0.12	12.7
131	42.0	0.13	18.9	1.54	0.11	13.5

TABLE A2 Experimental values obtained for I_{SC}, V_{OC}, P_M, I_M, and V_M as a function of G and T_c for the CdTe module

G [W/m²]	T_c [°C]	I_{SC} [A]	V_{OC} [V]	P_M [W]	I_M [A]	V_M [V]
1080	59.0	1.98	53.1	75.90	1.79	42.4
1001	55.6	1.82	52.8	71.29	1.65	43.3
1018	49.0	1.84	53.8	72.85	1.60	45.5
1000	45.1	1.81	53.9	72.56	1.62	44.7
953	37.9	1.72	54.0	69.22	1.53	45.2
1000	35.2	1.79	54.9	73.67	1.64	45.0
959	33.8	1.71	55.0	70.00	1.52	46.0
996	26.0	1.79	56.0	75.15	1.63	46.1
1002	25.4	1.77	55.8	75.24	1.62	46.4
759	56.8	1.39	51.8	52.54	1.24	42.4
802	45.0	1.44	52.9	56.40	1.28	44.0
738	28.8	1.31	54.5	53.48	1.18	45.3
300	36.0	0.54	50.8	20.48	0.49	42.1
261	50.6	0.47	48.7	16.09	0.42	38.5
161	55.8	0.30	46.4	9.76	0.26	38.1
152	35.8	0.27	48.6	8.80	0.24	36.8
198	28.1	0.35	50.2	13.20	0.32	41.5
145	27.8	0.26	49.1	9.20	0.23	40.0

TABLE A3 Values obtained for $I_{SC,\,ref}$, α, $V_{OC,\,ref}$, β, and k_G for the two modules characterized in the UAH. The RMSE for the estimation of I_{SC} and V_{OC} with respect to the experimental values is also included

	$I_{SC,ref}$ [A]	α [°C^{-1}]	RMSE I_{SC} [%]	$V_{OC,ref}$ [V]	β [°C^{-1}]	k_G [V^{-1}]	RMSE V_{OC} [%]
a-Si UAH	1.00	0.00053	0.88	23.21	−0.0038	0.08	0.35
CdTe UAH	1.78	0.00071	0.56	55.91	−0.0018	0.03	0.32

TABLE A4 Optimum values for n, $R_{sh,ref}$, and k_{Rsh} for the two modules characterized in the UAH and for 6 modules of [19]. G_{Rsh} has been set at 550 W/m². The RMSEs for the estimated P_M are also included

UAH modules	n	R_{sh} [Ω]	k_{Rsh} [m²/Ω]	RMSE [%]
a-Si UAH	1.8	2090	0.0050	0.16
CdTe UAH	1.5	750	0.0055	0.29
Reference [19]	n	R_{sh} [Ω]	k_{Rsh} [m²/Ω]	RMSE [%]
CdTe	1.8	950	0.0086	0.48
a-Si/a-Si/a-Si:Ge	4.8	60	0.0050	0.67
a-Si/a-Si:Ge	3.2	615	0.0039	0.50
CIS	1.7	120	0.0081	0.51
p-Si	1.2	125	0.0078	0.16
m-Si	1.2	155	0.0035	0.16

TABLE A5 RMSE obtained for P_M for the 8 modules considered (a-Si and CdTe measured in the UAH and the 6 of [18]). Both the errors using Equations (13a) and (13b) for R_s and those obtained with Equations (14a) and (14b) are shown. The RMSE obtained for each module with the Osterwald method (PTCM) is also included

	R_s Equations (13a) and (13b)	R_s Equations (14a) and (14b)	PTCM
UAH modules	**RMSE [%]**	**RMSE [%]**	**RMSE [%]**
a-Si UAH	1.22	1.24	7.16
CdTe UAH	0.95	0.92	2.46
	R_s Equations (13a) and (13b)	R_s Equations (14a) and (14b)	PTCM
Reference [18]	**RMSE [%]**	**RMSE [%]**	**RMSE [%]**
CdTe	1.30	1.43	1.68
a-Si/a-Si/a-Si:Ge	1.04	1.07	3.2
a-Si/a-Si:Ge	1.53	1.55	4.21
CIS	1.90	1.93	3.67
p-Si	1.18	1.27	1.15
m-Si	0.76	0.71	1.65
Average	1.24	1.27	3.15

TABLE A6 Optimum values for n, $R_{sh,ref}$, and k_{Rsh} calculated with the simple method described in section III.C for the two modules characterized in the UAH. G_{Rsh} has been set at 550 W/m². The RMSEs for the estimated P_M are also included

UAH modules	n	R_{sh} [Ω]	k_{Rsh} [m²/Ω]	RMSE [%]
a-Si UAH	1.8	2100	0.0055	1.23
CdTe UAH	1.5	750	0.0055	0.95